

Research paper

The influence of alkyl substitution on the in vitro metabolism and mutagenicity of benzo[a]pyrene

Danlei Wang^{a,*}, Angelique Groot^b, Albrecht Seidel^c, Lulu Wang^a, Effimia Kiachaki^a, Peter J. Boogaard^a, Ivonne M.C.M. Rietjens^a

^a Division of Toxicology, Wageningen University and Research, 6708WE, Wageningen, the Netherlands

^b Charles River Laboratories, Den Bosch BV, 5231 DD, 's-Hertogenbosch, the Netherlands

^c Biochemical Institute for Environmental Carcinogens, Prof. Dr. Gernot Grimmer-Foundation, 22927, Grosshansdorf, Germany

ARTICLE INFO

Keywords:

Alkylated B[a]P

Rat

Human

Microsomes

Mutagenicity

ABSTRACT

In recent years concerns over consumer exposure to mineral oil aromatic hydrocarbons (MOAH), especially those containing alkylated polycyclic aromatic hydrocarbons (PAHs), have emerged. This is especially due to the fact that some PAHs are known to be genotoxic and carcinogenic upon metabolic activation. However, available toxicological data on PAHs mainly relate to non-substituted PAHs with limited data on alkyl substituted PAHs. Therefore, the aim of the present study was to characterize in more detail the effect of alkyl substitution on the metabolism and mutagenicity of benzo[a]pyrene (B[a]P), a PAH known to be genotoxic and carcinogenic. To this end, the oxidative metabolism and mutagenicity of B[a]P and a series of its alkyl substituted analogues were quantified using in vitro microsomal incubations and the Ames test. The results obtained reveal that upon alkylation the metabolic oxidation shifts to the aliphatic side chain at the expense of aromatic ring oxidation. The overall metabolism, including metabolism via aromatic ring oxidation resulting potentially in bioactivation, was substantially reduced with elongation of the alkyl side chain, with metabolism of B[a]P with an alkyl substituent of >6 C atoms being seriously hampered. In the Ames test upon metabolic activation, the methyl substitution of B[a]P resulted in an increase or decrease of the mutagenic potency depending on the substitution position. The relevant pathways for mutagenicity of the selected monomethyl substituted B[a]P may involve the formation of a 7,8-dihydrodiol-9,10-epoxide, a 4,5-oxide and/or a benzylic alcohol as an oxidative side chain metabolite which subsequently may give rise to an unstable and reactive sulfate ester conjugate. It is concluded that alkylation of B[a]P does not systematically reduce its mutagenicity in spite of the metabolic shift from aromatic to side chain oxidation.

1. Introduction

The presence of parent (non-alkylated) and alkylated polycyclic aromatic hydrocarbons (PAHs) in mineral oils, raised safety concerns with respect to unintentional contamination of foodstuff and other consumer products with mineral oil aromatic hydrocarbons (MOAH) [1–4]. Legally accepted mineral oils applied in food production, in pharmaceuticals and cosmetic products are highly refined and non-carcinogenic, and generally referred to as highly refined base oils (HRBOs) or white mineral oils. Nonetheless, unintentional or illegal use of insufficiently refined mineral oils may result in contamination of foodstuffs, pharmaceuticals or cosmetics with polycyclic aromatics from mineral oils which can chromatographically be detected and are referred to as

MOAH. Some of these MOAH that can be detected in consumer products have been considered as potentially genotoxic and carcinogenic due to the presence of PAHs with 3–7 condensed rings with non or simple alkylation [5]. These PAHs generally need bioactivation to exert these adverse health effects. The present study focuses on benzo[a]pyrene (B[a]P) and a series of its alkylated analogues as model compounds to study the effect of alkylation on the in vitro metabolism and mutagenicity of PAHs. B[a]P is a typical mutagenic PAH that has been classified as a Group 1 carcinogen by the International Agency for Research on Cancer (IARC) based on evidence for its carcinogenicity in experimental animals and the consideration that the compound acts through a mechanism of carcinogenicity also relevant to humans [6]. Bioactivation of B[a]P and other non-substituted PAHs to their genotoxic

* Corresponding author. Division of Toxicology, Wageningen University and Research, PO Box 8000, 6700EA, Wageningen, the Netherlands.

E-mail address: danlei.wang@wur.nl (D. Wang).

<https://doi.org/10.1016/j.cbi.2022.110007>

Received 15 February 2022; Received in revised form 13 May 2022; Accepted 1 June 2022

Available online 6 June 2022

0009-2797/© 2022 The Authors. Published by Elsevier B.V. This is an open access article under the CC BY license (<http://creativecommons.org/licenses/by/4.0/>).

and carcinogenic metabolites was extensively studied in the past decades. These studies indicate that formation of a so-called bay region dihydrodiol-epoxide results in the most genotoxic and ultimate carcinogenic metabolite of these PAHs [7,8]. Fig. 1 presents the formation of such a bay region dihydrodiol-epoxide from B[a]P following conversion by cytochrome P450 (CYP450), microsomal epoxide hydrolase and again a CYP450-mediated reaction, ultimately resulting in the highly stereoselective formation of (+)-*anti*-B[a]P-7,8-dihydrodiol-9,10-epoxide (BPDE), one of four possible stereoisomers of B[a]P-7,8-dihydrodiol-9,10-epoxide, which is implied as an ultimate carcinogen of B[a]P [9]. Given that this pathway for bioactivation includes two CYP450-catalyzed monooxygenation steps, and that the presence of an alkyl substituent may redirect the CYP450-mediated conversion from aromatic to side chain oxidation [10], it remains to be elucidated whether alkylated bay-region PAHs would be bioactivated to a similar extent as the parent analogues. Given that the PAHs present in MOAH may in part represent alkylated PAHs the aim of the present study was to quantify the effect of alkyl substitution on the in vitro metabolism and genotoxicity of PAHs using B[a]P as the model compound.

Microsomal metabolic profiles for B[a]P and two of its methylated analogues are available in literature from the 1980s, including studies on 7-methyl-B[a]P [11–15], and 6-methyl-B[a]P [16,17]. These studies revealed that B[a]P is metabolized by rat or human liver microsomes and skin microsomes to dihydrodiols, quinones and phenols, specifically the 4,5-dihydrodiol, 7,8-dihydrodiol and 9,10-dihydrodiol of B[a]P, the 1,6-quinone, 3,6-quinone and 6,12-quinone of B[a]P, and 1-hydroxy-, 3-hydroxy- and 9-hydroxy-B[a]P (Fig. 2) [18–23]. The methylated analogue 7-methyl-B[a]P was reported to be converted by polychlorinated biphenyl (PCB)-induced rat liver microsomes to the same type of metabolites and, in addition, to the metabolite resulting from side chain oxidation, 7-hydroxymethyl-B[a]P (Fig. 2) [11–13]. Metabolic studies on the conversion of 6-methyl-B[a]P by 3-methylcholanthrene (3-MC)-induced rat liver microsomes suggested a similar profile of metabolites with additional formation of 1-hydroxy-6-hydroxymethyl-B[a]P, 3-hydroxy-6-hydroxymethyl-B[a]P, and an unidentified ring-hydroxylated 6-methyl-B[a]P (Fig. 2) [16,17]. These studies identified the various type of metabolites in a qualitative way but did not quantify the level of side chain versus aromatic hydroxylation, while they also did not include a comparison of B[a]P and its methylated analogues.

With respect to the mutagenicity it appeared that methyl substitution of B[a]P may increase or decrease the response in the Ames test. The limited number of reported studies on the effect of methylation on the mutagenicity and the dermal tumor-initiating activity of B[a]P are summarized in Table 1. The effect of monomethylation of B[a]P at twelve available carbon positions was examined in an Ames test with *S. typhimurium* tester strain TA100 in the studies of Chui et al. and Utesch et al. [24,25]. Although all tested monomethyl substituted B[a]P tested positive for mutagenicity towards TA100 upon metabolic activation with S9 homogenate [24–27], the mutagenic potency (expressed in

revertants/nmol) of each monomethyl substituted B[a]P varied between studies. In the study of Chui et al., the mutagenic potency of B[a]P and the monomethyl substituted B[a]Ps towards tester strain TA100 followed the order: 9-methyl-B[a]P > 4-methyl-B[a]P > 6-methyl-B[a]P > 11-methyl-B[a]P > B[a]P > another eight monomethyl substituted B[a]Ps that showed equal or less mutagenicity compared to B[a]P itself [24]. The study of Utesch et al. suggested the mutagenic potency to decrease in the order 4-methyl-B[a]P > B[a]P > other eleven monomethyl substituted B[a]Ps among the twelve monomethylated B[a]Ps tested in tester strain TA100 [25]. In line with the study of Chui et al., several other studies also reported 6-methyl-B[a]P being more mutagenic than B[a]P towards tester strain TA98 and TA100 [14,26–29]. No correlation between mutagenic potency in the Ames test and the skin tumor-initiating activity reported by Iyer et al. [30] was found for the twelve monomethyl substituted B[a]Ps.

The present study aims to provide novel biotransformation and mutagenicity data for several selected monomethyl substituted B[a]Ps, the latter towards both tester strains TA98 and TA100 that detect frameshift mutations and base-pair mutations, respectively. In particular, the effect of methyl substitution that may cause potentially different steric interactions with the involved metabolizing enzymes, on the possible underlying metabolic pathways and the resulting mutagenicity was explored. The reported studies suggested 6-methyl-B[a]P with a typically substituted *meso*-anthracenic position to be a more potent mutagen but a weaker skin tumor initiator than B[a]P. The distal substitution at the C3 position of B[a]P results in possibilities for a sterically undisturbed formation of a bay region dihydrodiol-epoxide apparently resulting in lower mutagenic potency but a stronger skin tumor-initiating activity than what was observed for B[a]P. Both the 7-methyl- and 8-methyl-B[a]P in which the methyl substituent may sterically block the formation of the bay region dihydrodiol-epoxide showed less or equal mutagenic potency compared to B[a]P, and appeared inactive in tumor initiation. Taken all together these data suggest that the monomethyl substitution of B[a]P at C3, C6, C7 or the C8 position provide interesting model compounds for metabolic and resulting mutagenicity studies among the twelve possible isomeric positions for substitution.

To better understand the oxidative metabolism mediated by CYP enzymes of alkyl-substituted and parent PAHs, the present study also characterizes the in vitro hepatic rat and human microsomal metabolism of an extended series of its alkylated analogues including in addition to B[a]P also 3-methyl-B[a]P, 6-methyl-B[a]P, 7-methyl-B[a]P, 8-methyl-B[a]P, 3-*n*-hexyl-B[a]P, and 3-*n*-dodecyl-B[a]P with the latter two being of special interest as synthetic model compounds for aromatic molecules bearing longer alkyl side chains and being suspected as genotoxic constituents within the group of MOAH.

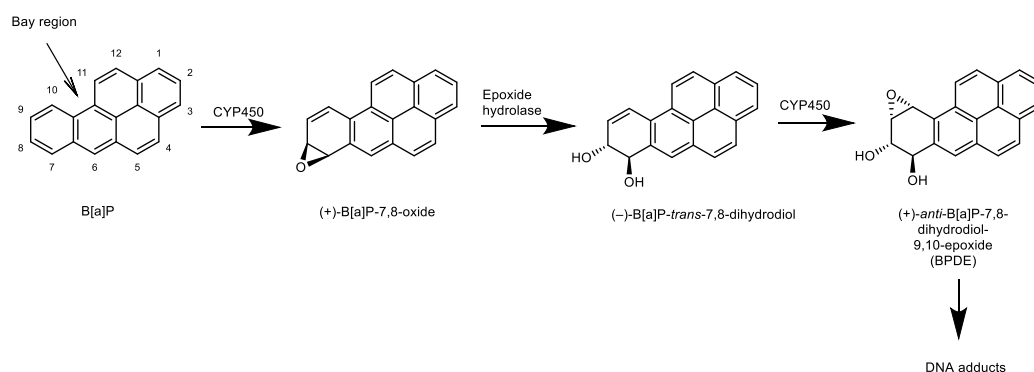


Fig. 1. Metabolic activation pathways of B[a]P to its ultimate genotoxic and carcinogenic metabolite.

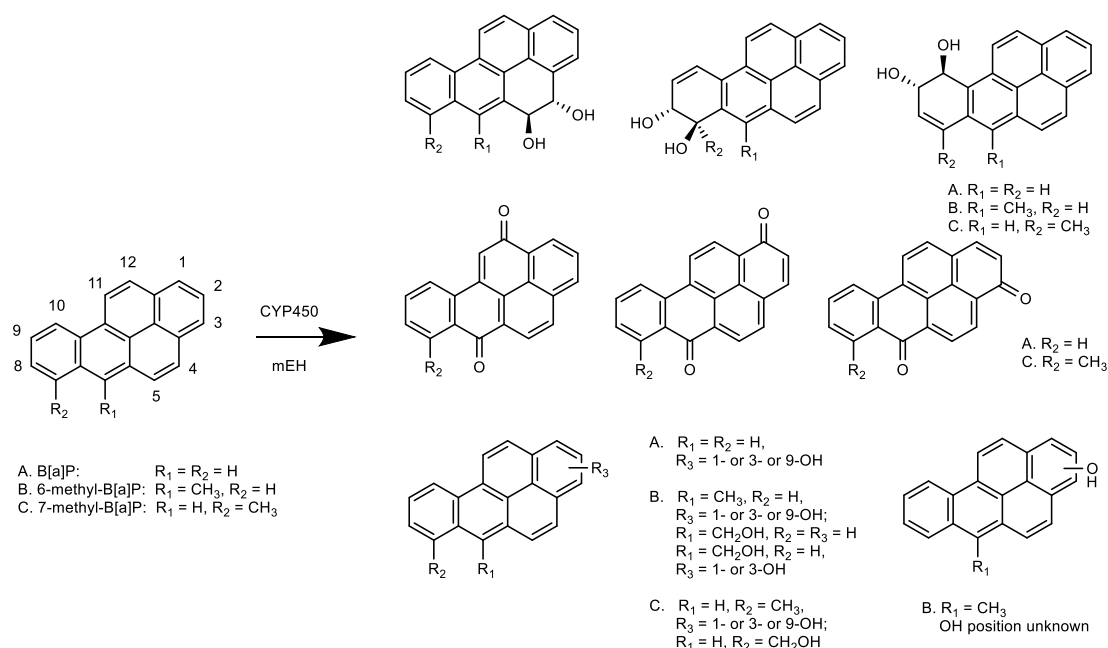


Fig. 2. A summary of the reported metabolites of B[a]P (A), 6-methyl- (B) and 7-methyl-B[a]P (C) formed by CYP450 enzymes and microsomal epoxide hydrolase (mEH) [11–13,16,17].

2. Material and methods

2.1. Chemicals and reagents

B[a]P ($\geq 99\%$), 7-methyl-B[a]P ($\geq 98\%$), 8-methyl-B[a]P ($\geq 98\%$), tetrahydrofuran ($\geq 99.9\%$), trifluoroacetic acid ($\geq 99\%$), methylmethanesulfonate (MMS), 2-aminoanthracene (2AA), and nitrofluorene (NF) were purchased from Sigma-Aldrich (St. Louis, USA). 3-Hydroxy-B[a]P was supplied by Toronto Research Chemicals (Toronto, Canada). 6-Methyl-B[a]P (99.5%) was obtained from CFW Laboratories (Newark, USA). 3-Methyl-B[a]P ($>99\%$), 6-hydroxymethyl-B[a]P ($>99\%$), 3-hydroxy-8-methyl-B[a]P ($>99\%$), 3-*n*-hexyl-B[a]P ($>99\%$), and 3-*n*-dodecyl-B[a]P ($>99\%$) were synthesized at the Biochemical Institute for Environmental Carcinogens (Großhansdorf, Germany). Acetonitrile was bought from Biosolve (Dieuze, France). Dimethyl sulfoxide (DMSO), $MgCl_2$, KCl and $K_2HPO_4 \cdot 3H_2O$ were supplied by Merck (Darmstadt, Germany). NADPH was obtained from Carbosynth (Berkshire, UK). GentestTM pooled male Sprague Dawley rat liver microsomes (RLM) and UltrapoolTM human liver microsomes (HLM), both with a protein concentration of 20 mg/ml were supplied by Corning (New York, USA), the latter containing cytochrome P450 liver enzymes of 150 individuals. Aroclor 1254 induced liver S9 homogenate prepared from male Sprague Dawley rats was obtained from Trinova Biochem GmbH (Giessen, Germany). *Salmonella typhimurium* TA98 and TA100 tester strains were also obtained from Trinova Biochem GmbH (Giessen, Germany). NADP and glucose-6-phosphate were supplied by Randox Laboratories Ltd. (Crumlin, UK) and Roche Diagnostics (Mannheim, Germany), respectively.

2.2. In vitro incubations of B[a]P and its alkylated congeners with rat and human liver microsomes

Microsomal incubations of B[a]P and its alkylated congeners with HLM and RLM consisted of 200 μ l incubations containing 0.1 M potassium phosphate (pH 7.4), 5 mM $MgCl_2$, HLM/RLM at a final microsomal protein concentration of 0.5 mg/ml, 1 mM NADPH, and each of the individual test compounds at concentrations ranging from 0 to 600 μ M. Test compounds were B[a]P, 3-methyl-B[a]P, 6-methyl-B[a]P, 7-methyl-B[a]P, 8-methyl-B[a]P, 3-*n*-hexyl-B[a]P and 3-*n*-dodecyl-B[a]P,

added from 100 times concentrated stock solutions in DMSO or tetrahydrofuran (the latter was used for 1-*n*-hexyl-B[a]P and 1-*n*-dodecyl-B[a]P due to their low solubility in DMSO). The final concentration of substrate solvent, in the incubation mixture was 1% (v/v), which is known to not affect the enzymatic activity of liver microsomes [31]. The incubation mixtures were prepared and incubated in glass tubes to avoid plastic binding of the substrates. After pre-incubation of the incubation mixture at 37 °C for 1 min, the enzymatic reaction was initiated by adding microsomes to the incubation mixture which was subsequently incubated at 37 °C for 30 min. Under these conditions metabolite formation was linear with the incubation time and the microsomal protein concentration (data not shown). Because the tested substrates and their metabolites bind to microsomal protein substantially, a diisopropylether (DIPE) extraction of the metabolites was performed after the reaction was stopped by the addition of 20 μ l 10% $HClO_4$. The sample was subsequently extracted three times with 1 ml DIPE. Each time, the upper layer was collected and the combined DIPE fractions were subsequently evaporated under a nitrogen stream. The residues were dissolved in 100 μ l methanol and analyzed by UPLC.

The metabolite concentrations were quantified by UPLC and used to calculate the rate of the enzymatic conversion in pmol/min/mg microsomal protein. The kinetic parameters K_M and V_{max} were obtained using a nonlinear regression (curve fit) applying the Michaelis Menten equation in GraphPad Prism 5 (San Diego, USA). The intrinsic clearance (Cl_{int}) was calculated as V_{max} divided by K_M and used to compare the metabolic efficiency for formation of the different metabolites.

2.3. UPLC analysis

The metabolites formed were analyzed and quantified using an Acquity UPLC system equipped with a photodiode array (PDA) detector (Waters, Milford, MA). The metabolites and their parent compound were separated on a reverse phase Acquity UPLC[®] BEH C18 column (21 \times 50 mm, 1.7 μ m, Waters, Milford, MA) and detected at a wavelength ranging from 190 nm to 400 nm. Eluent A was nano-pure water containing 0.1% trifluoroacetic acid (v/v), and eluent B was acetonitrile containing 0.1% trifluoroacetic acid (v/v). The gradient elution started from 90% A to 10% B applied from 0.0 min to 0.5 min, which was changed to 10% A and 90% B from 0.5 to 15.5 min and then kept at 10% A and 90% B from

Table 1

Overview of mutagenic potential of monomethyl substituted B[a]P and B[a]P itself in the Ames test as reported in the literature. Mutagenic potency was calculated from the initial ascending linear portion of the dose–response curve of each test compound (background subtracted), expressed as revertants per nmol. The tumor-initiating activity of the monomethyl substituted B[a]Ps and of B[a]P itself, assessed in the mouse skin painting assay, is expressed as percentage of mice with tumor. Note: the experimental conditions of bacterial reverse mutation assay may differ between studies. The studies for which the dose information was marked with “Not reported*” provided the mutagenic potency without presenting dose information.

Studies		Iyer et al. [30]	Bayless et al. [28]	Sullivan et al. [14]	Calle et al. [29]	Flesher et al. [27]		Santella et al. [26]	Chui et al. [24]	Utesch et al. [25]
		Tumor initiating activity (% mice with tumor)	No pre-incubation	No pre-incubation	No pre-incubation	No pre-incubation	No pre-incubation	No pre-incubation	Pre-incubation	Pre-incubation
			Single dose (nmoles/plate)	Not reported*	Single dose (nmoles/plate)	Not reported*		4 doses (0–10µg/plate)	4 doses (0–8µg/plate)	5 doses (0–100µg/plate)
			β-Naphthoflavone induced rat S9	β-Naphthoflavone induced rat S9	β-Naphthoflavone induced rat S9	Un-induced rat S9		1254 Aroclor induced mice S9	1254 Aroclor induced rat S9	Hepatocyte homogenate
			<i>S. typhimurium</i> strain							
			TA98	TA98	TA98	TA98	TA100	TA100	TA100	TA100
Compound	B[a]P	67 (Potent)	38 (6)	41	40 (6)	13	22	88	81	34
	1-Methyl-B[a]P	80 (Potent)	–	–	–	–	–	–	37	11
	2-Methyl-B[a]P	38 (Weak)	–	–	–	–	–	–	43	18
	3-Methyl-B[a]P	76 (Potent)	–	–	–	–	–	–	40	26
	4-Methyl-B[a]P	67 (Potent)	–	–	–	–	–	–	156	59
	5-Methyl-B[a]P	27 (Weak)	–	–	–	–	–	–	42	11
	6-Methyl-B[a]P	24 (Weak)	173 (2.8)	199	450 (0.94)	97	73	341	136	32
	7-Methyl-B[a]P	0 (Inactive)	–	14	–	–	–	37	85	14
	8-Methyl-B[a]P	3 (Inactive)	–	–	–	–	–	86	88	15
	9-Methyl-B[a]P	0 (Inactive)	–	–	–	–	–	60	178	15
	10-Methyl-B[a]P	0 (Inactive)	–	–	77 (2.9)	–	–	23	47	8
	11-Methyl-B[a]P	90 (Very potent)	–	–	–	–	–	111	116	24
12-Methyl-B[a]P	69 (Potent)	–	–	–	–	–	–	43	10	

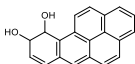
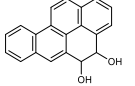
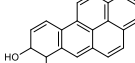
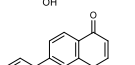
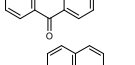
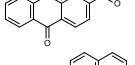
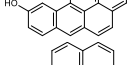
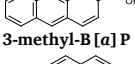
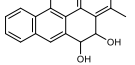
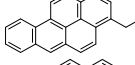
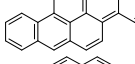
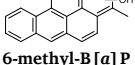
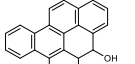
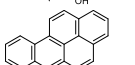
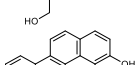
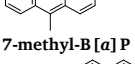
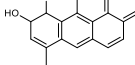
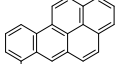
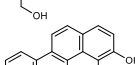
15.5 min to 18.5 min, changed back to 90% A and 10% B from 18.5 to 22.0 min. The total run time was 22 min using a flow rate of 0.6 ml/min. The temperature of the column was set at 40 °C and the autosampler at 10 °C during the UPLC analysis. The injection volume was 3.5 µl. Metabolites were quantified using their peak area at the wavelength specified in Table 2, using calibration curves of available reference compounds. Metabolites were identified by comparing their retention time (RT) and absorption spectra with those of reference standards. The unknown minor metabolites were tentatively identified and categorized by considering elution time on UPLC and GC-MS/MS, mass spectra and available elution and spectral information from literature as described in the result section.

2.4. Bacterial reverse mutation (Ames) assay

The mutagenicity of B[a]P and four of its methylated analogues including 3-methyl-B[a]P, 6-methyl-B[a]P, 7-methyl-B[a]P and 8-methyl-B[a]P was assessed in the bacterial reverse mutation (Ames) assay using *Salmonella typhimurium* strains TA98 and TA100. Six concentrations of each compound were tested in triplicate in the absence and presence of 5% (v/v) S9-mix obtained from the livers of Aroclor 1254 treated rats. The S9-mix contained 4 mM NADP, 5.8 mM glucose-6-phosphate, 0.1 M sodium phosphate pH 7.4, 8 mM MgCl₂, 33 mM KCl and 5% S9 homogenate. Fresh bacterial cultures were prepared overnight to reach 10⁹ cells/ml. Top agar was molten and heated at 45 °C. The following solutions were incubated at 70 rpm at 37 °C in a shaking water bath; either 0.5 ml S9-mix (in case of S9 presence) or 0.5 ml 0.1 M

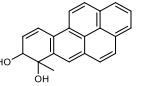
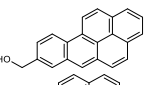
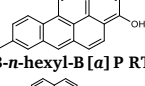
Table 2

The metabolite profile and corresponding Michaelis Menten parameters including K_M , V_{max} and C_{int} that was calculated as V_{max}/K_M . The results are shown as mean \pm standard error from three independent experiments. Abbreviations: RT = retention time; λ = wavelength of maximum UV absorbance of the compound; ND = not detected; NM = no metabolism.

Metabolites	Structure	Species	K _M (μM)	V _{max} (pmol/min/mg microsomal protein)	C _{int} (V _{max} /K _M) μl/min/mg protein
B[a]P RT = 10.66min, λ = 296.4 nm					
9,10-dihydro-B[a]P-diol RT = 4.65min, λ = 278.6 nm;		HLM	12.2 ± 8.5	3.8 ± 0.6	0.2
		RLM	11.9 ± 5.5	28.3 ± 2.8	2.4
4,5-dihydro-B[a]P-diol RT = 5.69min, λ = 273.1 nm		HLM	15.0 ± 11.8	4.6 ± 0.9	0.2
		RLM	6.5 ± 4.5	13.3 ± 1.4	2.0
7,8-dihydro-B[a]P-diol RT = 5.79min, λ = 296.4 nm		HLM	ND	ND	–
		RLM	14.6 ± 9.8	7.0 ± 1.1	0.5
7,8-dihydro-B[a]P-diol RT = 5.90min, λ = 367.4 nm;		HLM	ND	ND	–
		RLM	12.6 ± 10.7	13.3 ± 2.5	1.1
B[a]P-1,6-quinone RT = 6.64min, λ = 219.4 nm;		HLM	ND	ND	–
		RLM	14.8 ± 8.8	22.2 ± 3.2	1.5
B[a]P-3,6-quinone RT = 7.19min, λ = 223.7 nm;		HLM	ND	ND	–
		RLM	24.0 ± 14.4	3.0 ± 0.5	0.1
9-hydroxy-B[a]P RT = 8.22min, λ = 267.6 nm;		HLM	ND	ND	–
		RLM	11.4 ± 5.2	20.0 ± 1.9	1.8
3-hydroxy-B[a]P RT = 8.51min, λ = 258.4 nm;		HLM	26.4 ± 25.9	27.0 ± 9.1	1.0
		RLM	12.7 ± 3.5	99.5 ± 6.1	7.8
3-methyl-B[a]P RT = 11.45min, λ = 301.9 nm					
4,5-dihydro-3-methyl-B[a]P-diol RT = 4.74min, λ = 273.7 nm;		HLM	ND	ND	–
		RLM	28.8 ± 5.9	2.7 ± 0.2	0.1
3-hydroxymethyl-B[a]P RT = 7.83min, λ = 301.3 nm;		HLM	15.4 ± 7.9	3.6 ± 0.5	0.2
		RLM	2.9 ± 3.3	25.0 ± 3.4	8.6
3-B[a]P-carbaldehyde RT = 7.98min, λ = 226.1 nm;		HLM	87.0 ± 38.1	6.4 ± 1.3	0.1
		RLM	149.3 ± 19.4	42.4 ± 3.1	0.3
Hydroxy-3-methyl-B[a]P RT = 9.24min, λ = 256.6 nm;		HLM	58.3 ± 12.8	12.0 ± 1.1	0.2
		RLM	137.4 ± 23.0	26.4 ± 2.4	0.2
6-methyl-B[a]P RT = 11.35min, λ = 300.0 nm					
4,5-dihydro-6-methyl-B[a]P-diol RT = 4.81min, λ = 273.1 nm		HLM	ND	ND	–
		RLM	2.8 ± 1.8	2.8 ± 0.2	1
6-hydroxymethyl-B[a]P RT = 7.68min, λ = 299.4 nm		HLM	168.8 ± 117	30.8 ± 12.4	0.2
		RLM	71.2 ± 19.7	35.0 ± 4.2	0.5
3-hydroxy-6-methyl-B[a]P RT = 9.28min, λ = 264.5 nm		HLM	6.6 ± 8.8	3.2 ± 0.7	0.5
		RLM	5.4 ± 9.1	3.8 ± 0.9	0.7
7-methyl-B[a]P RT = 11.34min, λ = 298.2 nm					
9,10-dihydro-7-methyl-B[a]P-diol RT = 5.1min, λ = 276.7 nm		HLM ^a	3.0 ± 3.7	0.3 ± 0.0	0.1
		RLM	ND	ND	–
7-hydroxymethyl-B[a]P RT = 7.8min, λ = 297.6 nm		HLM ^a	3.2 ± 3.1	1.3 ± 0.1	0.4
		RLM	7.9 ± 12.0	49.9 ± 18.0	6.3
3-hydroxy-7-methyl-B[a]P RT = 9.15min, λ = 268.2 nm		HLM ^a	3.4 ± 4.1	2.7 ± 0.3	0.8
		RLM	3.4 ± 11.5	32.3 ± 10.4	9.5
8-methyl-B[a]P RT = 11.53min, λ = 297.6 nm					
4,5-dihydro-8-methyl-B[a]P-diol RT = 4.07min, λ = 274.9 nm;		HLM	ND	ND	–
		RLM	3.3 ± 7.3	3.1 ± 0.7	0.9

(continued on next page)

Table 2 (continued)

Metabolites	Structure	Species	K_M (μ M)	V_{max} (pmol/min/mg microsomal protein)	Cl_{int} (V_{max}/K_M) μ l/min/mg protein
7,8-dihydro-8-methyl-B[a]P-diol RT = 5.56min, λ = 259 nm;		HLM	ND	ND	–
7,8-dihydro-8-methyl-B[a]P-diol RT = 5.62min, λ = 259 nm;		RLM	2.9 ± 5.1	5.2 ± 1.4	1.8
		HLM	ND	ND	–
		RLM	4.8 ± 6.5	3.4 ± 1.1	0.7
8-hydroxymethyl-B[a]P RT = 7.87min, λ = 298.2 nm;		HLM	29.1 ± 23.3	13.2 ± 3.3	0.5
		RLM	8.4 ± 5.2	418.8 ± 47.2	49.9
3-hydroxy-8-methyl-B[a]P RT = 9.33min, λ = 258.4 nm;		HLM	64.7 ± 66.5	14.7 ± 6.4	0.2
		RLM	11.6 ± 8.4	68.8 ± 10.7	5.9
	3-n-hexyl-B[a]P RT = 14.25min, λ = 302.5 nm				
Dihydro-3-n-hexyl-B[a]P-diol RT = 4.70min, 247.4 nm		HLM	36.0 ± 49.4	1.5 ± 0.7	0.04
		RLM	36.7 ± 13.1	1.3 ± 0.2	0.04
	3-dodecyl-B[a]P RT = 17.45min, λ = 301.9 nm				
NM	–	HLM	–	–	–
NM	–	RLM	–	–	–

^a The data marked HLM with 7-methyl-B[a]P were obtained following 5 h incubation.

phosphate pH 7.4 (in case of S9 absence), mixed with 0.1 ml of a fresh bacterial culture (10^9 cells/ml) of TA98 or TA100, and 2.5–25 μ g test compound per plate. After incubation, the solutions were added to 3 ml molten top agar and mixed with vortexing. The content of the top agar tube was poured onto a minimal glucose agar plate. After solidification of the top agar, the plates were incubated at 37 °C for 48 h. The number of revertant colonies per plate was automatically counted with the Instem Sorcerer Colony Counter (Staffordshire, UK). In the absence of S9-mix, NF (10 μ g/plate) and MMS (650 μ g/plate) were tested as positive controls for incubations with TA98 and TA100, respectively. In the presence of S9-mix, 2AA (1 μ g/plate and 5 μ g/plate) was tested as a positive control in both TA98 and TA100. DMSO was tested as a solvent

control in both tester strains. The results are considered biologically relevant for mutagenic potential when the induced increases in the number of revertant colonies are above the historical control database and more than 3-fold or 2-fold higher than concurrent controls for tester strains TA98 and TA100, respectively [32].

To obtain insight in the nature of the metabolites generated, additional incubations with the S9 mix were performed and analyzed as described above for the microsomal incubations. These S9 incubations had the same composition as the mixture that the bacteria were exposed to in the Ames test, and consisted of 150 μ M (20 μ g) test compound, 500 μ l S9-mix (in the presence of metabolic activation) or 0.1 M sodium phosphate (pH 7.4) (in the absence of metabolic activation). The

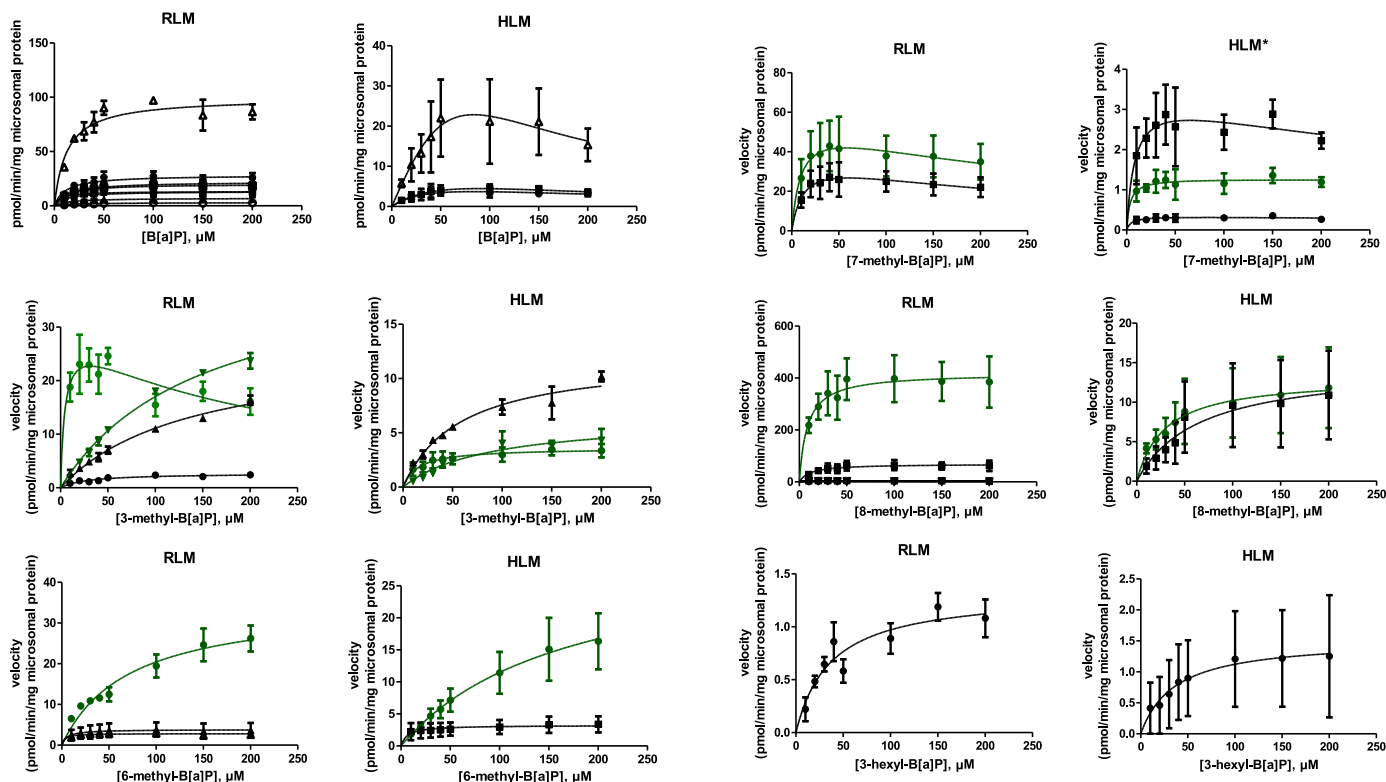


Fig. 3. Substrate concentration dependent metabolite formation for B[a]P and its alkyl substituted analogues by non-induced RLM and HLM. Black curves represent formation of metabolites resulting from aromatic ring oxidation and green curves present formation of metabolites resulting from alkyl side chain oxidation. Each symbol represents experimental means and vertical bars are standard errors of the mean ($n = 3$).

Note: The Y-axis varies between the presented figures. * The figure of 7-methyl-B[a]P by HLM was obtained following 5 h instead of 30min incubation.

mixture was incubated at 37 °C for 48 h and subsequently treated and analyzed for metabolites formed as described above in section 2.2 and 2.3 for the microsomal incubations.

3. Results

3.1. Microsomal metabolism of B[a]P and alkyl substituted B[a]Ps

The kinetics of substrate concentration dependent metabolism mediated by hepatic P450 enzymes of rat and human are shown in Fig. 3. The results obtained reveal that while most of the metabolite formations followed Michaelis Menten type saturation kinetics, in some cases substrate inhibition was observed at higher concentrations. By fitting the data to the Michaelis Menten equation, the kinetic parameters including K_M , V_{max} and Cl_{int} for formation of each metabolite were obtained and are presented in Table 2.

For the metabolites showing substrate inhibition, the K_M and V_{max} presented in Table 2 were obtained from Michaelis Menten fitting approach with exclusion of the concentrations that showed inhibition.

The metabolites formed upon rat microsomal metabolism of B[a]P were identified and characterized in our recently published paper [19]. Compared to RLM, a lower number of metabolites appeared to be formed following metabolism mediated by P450 enzymes from HLM. In HLM, two dihydrodiols and a phenolic metabolite were identified as 9,10-dihydro-B[a]P-diol, 4,5-dihydro-B[a]P-diol and 3-hydroxy-B[a]P eluting at 4.65 min, 5.69 min, and 8.51 min, respectively. 7,8-Dihydro-B[a]P-diol, quinones and 9-hydroxy-B[a]P that were formed in RLM incubations were not detected in the microsomal incubation of B[a]P with HLM. Methyl substitution of B[a]P generally shifted the oxidative metabolism to the methyl side chain in incubations with both RLM and HLM. Besides the formation of dihydrodiols and phenols, side chain alcohol metabolites become the most abundant metabolites in incubations of the methyl substituted B[a]Ps with RLM but not necessarily with HLM (Fig. 3, Table 2).

The primary metabolite, eluting at 7.68 min, that was formed in incubations of 6-methyl-B[a]P with both RLM and HLM, was characterized as 6-hydroxymethyl-B[a]P by co-elution and the same UV spectrum as that of the synthesized reference chemical. A phenolic metabolite was detected at a retention time of 9.59 min and identified as 3-hydroxy-6-methyl-B[a]P based on a similar UV spectrum as 3-hydroxy-B[a]P and 3-hydroxy-8-methyl-B[a]P. The 4,5-dihydro-6-methyl-B[a]P-diol, eluting at 4.81 min, was identified as the only dihydrodiol formed in the incubations of 6-methyl-B[a]P with RLM based on the reported spectrum of a synthetic reference standard [16]. No dihydrodiols of 6-methyl-B[a]P were formed in the incubation with HLM.

7-Methyl-B[a]P was metabolized to 7-hydroxymethyl-B[a]P and 3-hydroxy-7-methyl-B[a]P; both metabolites could be identified based on similarity of their reported elution and UV spectra to 7-hydroxymethyl-B[a]P and 3-hydroxy-7-methyl-B[a]P [11]. 7-Methyl-B[a]P was not metabolized by HLM after 30 min incubation. Upon prolonged 5 h incubation with HLM, besides 7-hydroxymethyl-B[a]P and 3-hydroxy-7-methyl-B[a]P, an additional metabolite was detected at a retention time of 5.1 min, which was identified as 9,10-dihydro-7-methyl-B[a]P-diol based on the spectral similarity to 9,10-dihydro-B[a]P-diol and the reported UV spectrum of 9,10-dihydro-7-methyl-B[a]P-diol [11].

In RLM incubations of 8-methyl-B[a]P, three dihydrodiols eluting at 4.07 min, 5.56 min, and 5.62 min, respectively, were identified as 8-methyl-B[a]P-4,5-dihydrodiol and 8-methyl-B[a]P-7,8-dihydrodiols by comparison of their UV spectra to that of B[a]P-dihydrodiols and the reported UV spectra of 8-methyl-B[a]P-7,8-dihydrodiol [33]. No diols were formed in incubations of 8-methyl-B[a]P with HLM. The most abundant metabolite, eluting at 7.87 min, was identified as 8-hydroxymethyl-B[a]P. The metabolite formed in both RLM and HLM with a retention time of 9.33 min was characterized as 3-hydroxy-8-methyl-B[a]P based on comparison of its elution time and UV spectrum to the synthesized reference chemical.

Metabolite identification of 3-methyl-B[a]P was based on the comparison of retention time and UV spectrum of the metabolites to those of other methyl substituted B[a]Ps. The metabolite eluting at 4.74 min was identified tentatively as 3-methyl-B[a]P-4,5-dihydrodiol based on its UV spectrum similarity to the spectrum of 4,5-dihydrodiol-B[a]P. The metabolite at a retention time of 7.81 min was identified as 3-hydroxymethyl-B[a]P based on the effect of the hydroxylation on the retention time and UV spectrum, that was comparable to the effect of hydroxylation on the retention time and UV spectrum observed for 6-hydroxymethyl-B[a]P as compared to 6-methyl-B[a]P. The metabolite eluting at 7.95 min was tentatively identified as 3-B[a]P-carbaldehyde, eluting next to 3-hydroxymethyl-B[a]P, based on the elution pattern of 1-naphthylmethylketone that was reported to elute close to 1-(1-hydroxyethyl)-naphthalene [10].

In the incubation of 3-*n*-hexyl-B[a]P with RLM and HLM, a common metabolite was formed eluting at 4.70 min that was tentatively identified as a dihydrodiol of 3-*n*-hexyl-B[a]P for eluting in the dihydrodiol region. This dihydrodiol metabolite is possibly the 4,5-dihydrodiol of 3-*n*-hexyl-B[a]P based on the similarity of its UV spectrum to the spectrum of 4,5-dihydro-3-methyl-B[a]P-diol. 3-*n*-Dodecyl-B[a]P was metabolized by neither HLM nor RLM under the experimental conditions applied.

3.2. Intrinsic clearance via side chain oxidation versus aromatic ring oxidation for B[a]P and alkyl substituted B[a]Ps

The intrinsic clearance of B[a]P and its alkylated analogues via the different metabolites was summed up based on whether the metabolite formation represents side chain or aromatic oxidation of the tested model compounds (Fig. 4). Generally, methyl substitution of B[a]P shifted the metabolism to methyl side chain oxidation at the cost of aromatic ring oxidation. In incubations with RLM, the intrinsic clearance via aromatic ring oxidation of the methyl substituted B[a]Ps was 1.8- to 57.0- fold lower than what was observed for B[a]P itself. Side chain oxidation of 3-methyl-B[a]P and 8-methyl-B[a]P becomes the dominant pathway and was 29.7- and 5.3- fold higher than that observed for aromatic ring oxidation with respect to the intrinsic clearance. However, intrinsic clearance of 6-methyl- and 7-methyl-B[a]P in incubations with RLM via aromatic ring oxidation was 3.4- fold and 1.5- fold lower than via the side chain oxidation. In incubations with HLM the intrinsic clearance of aromatic ring oxidation of alkylated B[a]Ps was 2.8- to 7- fold lower compared to the that of B[a]P itself, except for 7-methyl-B[a]P for which the overall conversion by HLM within the 30-min incubation appeared not to result in detectable metabolite formation. The intrinsic clearance of 3-methyl- and 8-methyl- B[a]P via side chain oxidation was 2.2- to 2.5- fold higher than that via aromatic ring oxidation. However, for 6-methyl-B[a]P metabolism via side chain oxidation was 2.5- fold lower than that via aromatic ring oxidation. 1-*n*-Hexyl-B[a]P was oxidized via only aromatic ring oxidation with the intrinsic clearances via aromatic ring oxidation being 430.0- and 35.0- fold lower than for B[a]P itself with RLM and HLM respectively.

3.3. Overall intrinsic clearance of B[a]P and its alkyl substituted B[a]Ps via cytochrome P450 mediated metabolism

The overall efficiency of the liver microsomal metabolism of B[a]Ps, calculated as the sum of side chain and aromatic oxidation, appeared to depend on the species, the position of the alkyl substitution and the length of the alkyl chain. This total intrinsic clearance of B[a]P and its alkylated analogues was calculated and summarized in Fig. 5. The intrinsic metabolic clearance of B[a]P by RLM was 12.3-fold higher than that observed for HLM. For the series of methylated B[a]P substrates liver microsomal metabolism by RLM was 3.1- to 84.7- fold more efficient than that observed for HLM, with the difference being greatest for 8-methyl-B[a]P. With the exception of 8-methyl-B[a]P that was metabolized 3.4- fold faster than the parent PAH by RLM, for all other

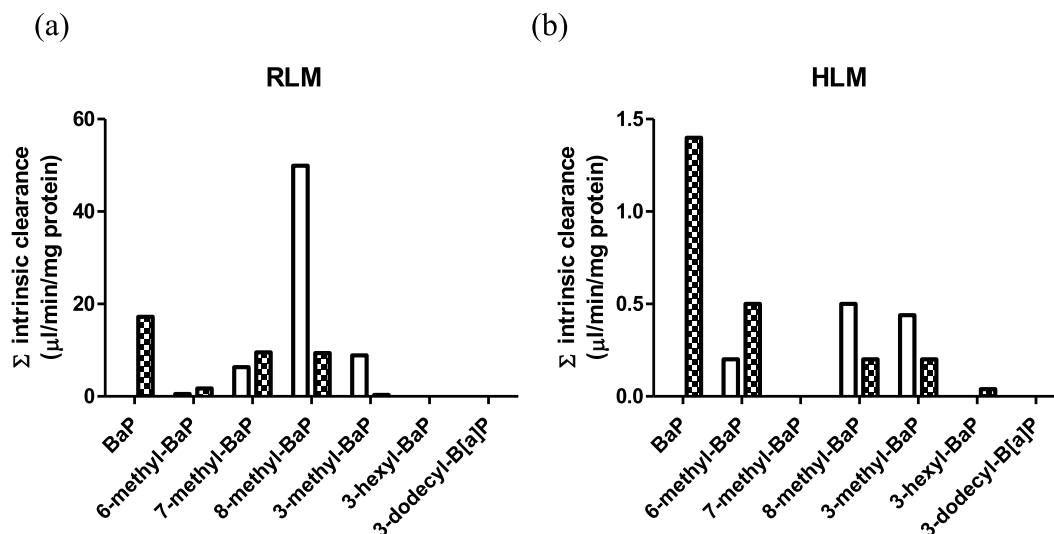


Fig. 4. Intrinsic clearance via aromatic ring oxidation versus alkyl side chain oxidation mediated by (a) RLM and (b) HLM for B[a]P and its alkylated analogues. Aromatic ring oxidation; alkyl chain oxidation. Note: the Y-axis varies between the presented figures.

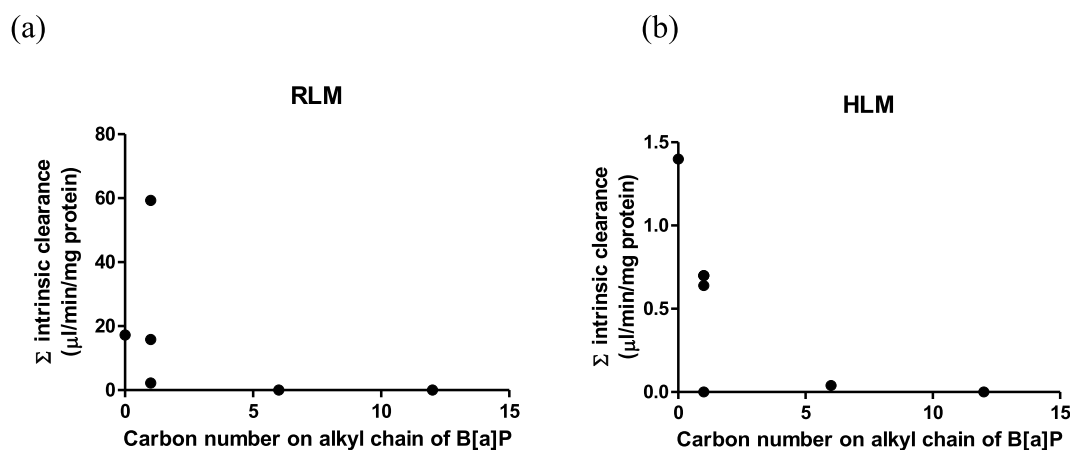


Fig. 5. Overall intrinsic clearance of alkyl-substituted B[a]Ps in metabolism with (a) RLM (b) HLM based on the number of carbon atoms in the alkyl side chain. Note: the Y-axis varies between the presented figures.

alkylated B[a]P model compounds tested metabolism was substantially less, being 1.1- to 430.0-fold lower, than what was observed for B[a]P itself. For HLM mediated metabolism, besides that 7-methyl-B[a]P was not metabolized to a detectable extent, other alkyl substituted B[a]P with alkyl chains up to and including 6 carbon atoms, were metabolized 2.0- to 35.0-fold slower than B[a]P itself. By extending the incubation time to 5 h, 7-methyl-B[a]P was metabolized with an overall intrinsic clearance of 1.3 $\mu\text{l/min/mg protein}$ by HLM. The alkyl chain length also appeared to play a role in the overall clearance via cytochrome P450 mediated conversion, since no conversion of 3-*n*-dodecyl-B[a]P was detected even after 5 h incubation, neither with RLM nor with HLM.

3.4. Mutagenicity of B[a]P and its methyl analogues

At the tested doses of the methyl-substituted B[a]Ps and B[a]P itself, no precipitation of the compounds was observed in the Ames test. Cytotoxicity and abnormal bacterial background lawn were also not observed for all tested compounds. The dose response curves of each test compound are depicted with doses ($\mu\text{g/plate}$) against observed number of revertants (His^+) in TA98 and TA100 in the presence of S9 metabolic activation in Fig. 6a and Fig. 6b, respectively. The mutagenic efficacy (fold induction), calculated from the maximum increase in the number of revertants divided by the number of revertants for the solvent control,

was used to judge the mutagenicity of the test compound based on the 3-fold and 2-fold criteria for TA98 and TA 100, respectively. It is concluded that B[a]P and its four methyl substituted analogues tested positive in the presence of S9 metabolic activation in both tester strains (Table 3). An estimate of the mutagenic potency (revertants/nmol), calculated from the initial ascending linear tendency of the dose-response curve of each test compound, is presented in Table 3, and was used to assess the mutagenic potential of the test compounds. The observed effect of methyl substitution of B[a]P on its mutagenic potency follows the order: 6-methyl-B[a]P > B[a]P > 8-methyl-B[a]P = 7-methyl-B[a]P > 3-methyl-B[a]P towards tester strain TA98; and 3-methyl-B[a]P > 8-methyl-B[a]P > 7-methyl-B[a]P > B[a]P > 6-methyl-B[a]P towards tester strain TA100 (Table 3). The observed results suggest that the effect of monomethyl substitution on the mutagenic potency of B[a]P depends on the position of the substitution and the tester strain used.

3.5. Liver S9 mediated metabolism B[a]P and methyl substituted B[a]Ps

Given that in the Ames test an S9 metabolic activation system was used, the metabolite profiles of B[a]P and its methylated analogues that were tested in the Ames test were also characterized upon incubations that matched the incubation conditions of the Ames test. The

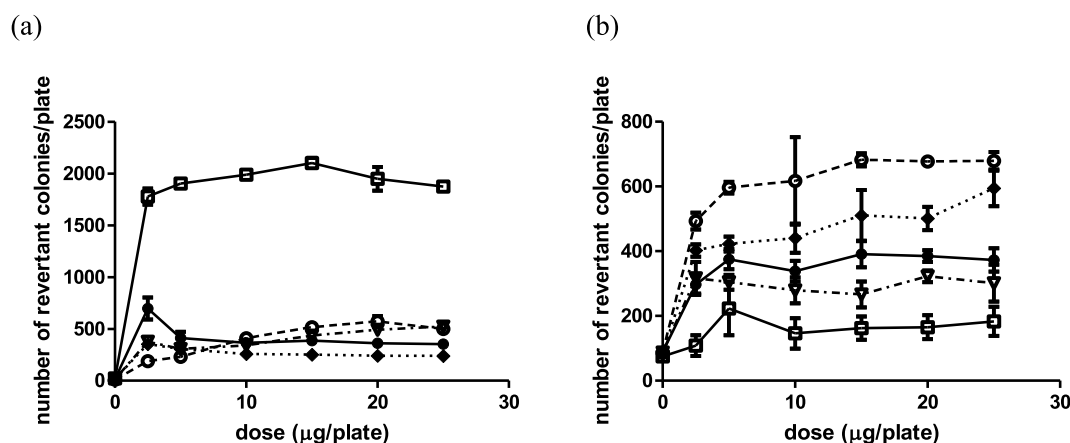


Fig. 6. Number of revertants in *S. typhimurium* (a) TA98 (b) TA100 upon exposure to (●) B[a]P, (●) 3-methyl-B[a]P, (■) 6-methyl-B[a]P, (▼) 7-methyl-B[a]P and (◆) 8-methyl-B[a]P in the presence of 5% S9-mix. Each symbol represents a mean and vertical bars are the standard deviations of the mean ($n = 3$). The mean number of revertant colonies per plate ($n = 15$) of solvent control was 15 ± 5 and 12 ± 4 with and without S9-mix (1254 Aroclor induced rat S9) in tester strain TA98, respectively. 1 $\mu\text{g}/\text{plate}$ 2AA with S9-mix and 10 $\mu\text{g}/\text{plate}$ NF without S9-mix that were tested as positive controls towards tester strain TA98 resulted in 532 ± 59 and 1343 ± 117 revertants per plate, respectively. The mean number of revertant colonies per plate ($n = 15$) of solvent control was 84 ± 8 and 111 ± 7 with and without S9-mix in tester strain TA100, respectively. 5 $\mu\text{g}/\text{plate}$ 2AA with S9-mix and 650 $\mu\text{g}/\text{plate}$ MMS without S9-mix that were tested as positive controls towards tester strain TA100 resulted in 1368 ± 168 and 653 ± 67 revertants per plate, respectively.

Table 3

Mutagenicity of B[a]P and its monomethyl substituted analogues in the Ames test with *S. typhimurium* TA98 and TA100 in the presence of Aroclor 1254 induced rat liver S9 and NADPH-generating system. Mutagenic efficacy of each compound was calculated as the fold induction from the maximum increase in the number of revertants through dividing by the number of revertants in the solvent controls. Mutagenic potency of each compound was the maximum value of the calculated values from the net increase in number of revertants divided by the dose, expressed as revertants per nmol.

Compound	<i>S. typhimurium</i> strain			
	TA98		TA100	
	Mutagenic efficacy	Mutagenic potency	Mutagenic efficacy	Mutagenic potency
B[a]P	44	69	4.9	21
3-methyl-B[a]P	57	19	7.9	43
6-methyl-B[a]P	100	187	3	3.5
7-methyl-B[a]P	40	39	3.7	24
8-methyl-B[a]P	24	39	7.2	34

chromatograms presenting the metabolic profiles of the test compounds following incubation for 48 h with 1254 Aroclor induced liver S9-mix used in the Ames test are presented in Fig. S1 (supplementary material). In line with the metabolites formed in the microsomal incubations, also in the incubation of B[a]P with S9-mix, dihydrodiols, quinones and phenols were formed as primary metabolites. In the S9 incubations, the

metabolism of monomethyl substituted B[a]Ps again generally shifted to side chain oxidation with other metabolites including dihydrodiols, quinones and phenols being formed to a lower extent. The concentration of especially three types of dihydrodiol metabolites formed in the S9 incubations of B[a]P and its monomethylated analogues (substrate concentration 150 μM that is equivalent to the dose of 20 μg in Ames

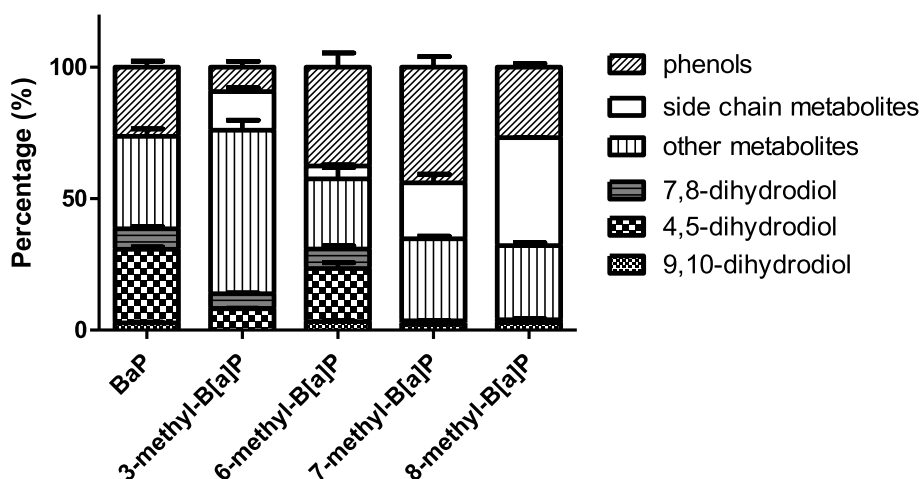


Fig. 7. Percentage (%) of the different metabolites in the total metabolite pattern in 1254 Aroclor induced rat S9 incubations with B[a]P and four of its methyl substituents, calculated from the concentration of the metabolite divided by the total concentration of metabolites. Each bar represents experimental means and vertical bars are standard errors of the mean ($n = 3$). The absolute concentration (μM) of the metabolites of each test compound is presented in Fig. S2 (supplementary materials).

test) was quantified and is presented in Fig. 7. The total concentration of the formed metabolites varies between the methylated analogues (Fig. S2 in supplementary material). The total concentration of the formed metabolites in the S9 incubation of B[a]P was $14.2 \pm 6.6 \mu\text{M}$ which was 2.4- fold, 3.7- fold, and 2.5- fold higher than the total metabolite formation for 3-methyl-, 6-methyl- and 7-methyl-B[a]P, respectively, while being 1.4- fold lower than that of 8-methyl-B[a]P (Fig. S2). Formation of 4,5-dihydrodiol was found to be abundant in S9 incubations of B[a]P, 3-methyl- and 6-methyl-B[a]P at levels amounting to 28%, 8% and 20% of the total metabolite formation while only 0.3% and 1.1% of 4,5-dihydrodiol was found in the S9 incubations of 7-methyl- and 8-methyl-B[a]P (Fig. 7). In the S9 incubations, 7,8-dihydrodiol metabolites were formed at levels amounting to 7.8%, 5.8%, 7.4%, 1.0% and 0% of the total formation of metabolites for B[a]P, 3-methyl-, 6-methyl-, 7-methyl- and 8-methyl-B[a]P, respectively. Formation of 9,10-dihydrodiol in the S9 incubations was on average 2.2–3.0% of the total metabolite formation for B[a]P and its monomethylated analogues, except for the fact that 9,10-dihydrodiol was not formed from 3-methyl-B[a]P.

4. Discussion

The emerging concern of consumption of polycyclic aromatics, that are detectable as MOAH, via food, pharmaceuticals and cosmetics relates mainly to 3- to 7- ring PAHs with no or simple alkylation, which can possibly induce genotoxicity and carcinogenicity. So far, especially metabolism and genotoxicity of unsubstituted PAHs like B[a]P were studied, while the effect of alkylation, in particular with longer side chains, of PAHs on their mutagenic and carcinogenic potential and relevant bioactivation pathways is far less characterized. This study investigated the effect of alkyl substitution on the in vitro metabolism and genotoxicity of B[a]P. The results obtained provide support for the hypothesis that alkylation of B[a]P shifts oxidative metabolism mediated by CYP450 enzymes to alkyl side chain oxidation at the expense of aromatic ring oxidation. This was the case in incubations with both non-induced RLM and HLM. A similar shift in favor of side chain oxidation at the expense of aromatic ring oxidation was previously observed for naphthalene and phenanthrene and their alkylated analogues [10,34]. As genotoxicity and carcinogenicity of B[a]P, and also its developmental toxicity, are considered to require metabolic activation to aromatic ring oxidative metabolites [8,19,35], the observed metabolic shift to side chain oxidation at the expense of aromatic ring oxidation may point at lower chances of bioactivation. The results also elucidated that with an increase of the alkyl chain length the extent of metabolism, including also metabolism via aromatic ring oxidation and thus bioactivation, was also substantially reduced. This was reflected by the limited overall

metabolic efficiency for conversion of 3-*n*-hexyl-B[a]P that was 430- and 35- fold lower than that of B[a]P in incubations with the non-induced RLM and HLM, respectively, and the fact that metabolic conversion of 3-*n*-dodecyl-B[a]P was not observed at all. These observations are also in line with the metabolic pattern that was observed for alkylated naphthalenes and phenanthrenes [10,34], and might be ascribed to steric hindrance hampering adequate binding of the alkylated PAHs to the active site of the CYP450 enzymes involved. The observed limited metabolic conversion of 3-*n*-dodecyl-B[a]P seems in line with the negative mutagenic potential of an octadecyl substituted B[a]P derivative in the reverse mutation assay [36].

It is also of interest that, in addition to these overall effects of alkyl substitution on the metabolic profiles of B[a]P and its methylated congeners, also some differences in metabolic profile were observed between incubations with RLM and HLM. Incubation of B[a]P and monomethylated B[a]Ps with RLM generated metabolites at higher catalytic efficiency and also generated more types of metabolites, including especially a higher level of dihydrodiols than what was observed in incubations with HLM. Assuming that some dihydrodiols may represent proximate mutagenic metabolites (Fig. 1), the absence of their formation at detectable levels in incubations with HLM but not with RLM may reflect a minor contribution of this route for bioactivation by HLM than RLM.

B[a]P and the selected monomethylated analogues tested positive for mutagenicity upon metabolic activation with 1254 Aroclor induced rat S9 in the Ames test. The mutagenic potency (revertants/nmol) of B[a]P, 3-methyl-, 6-methyl-, 7-methyl- and 8-methyl-B[a]P towards both tester strains TA98 and TA100 is summarized across the present and historical studies in Fig. 8 [14,24–29]. The overview thus obtained reveals that the methylated B[a]P analogues generally show a mutagenic potency that is within a factor of 3-fold similar to that of B[a]P with the exception of 6-methyl B[a]P, in which the substituent is positioned at C6 (meso position), and which appeared to be more potent especially in tester strain TA98 that detects frameshift mutations, while in tester strain TA100 that detects base-pair substitutions, the results appear more variable. Part of the differences in mutagenic potency may be ascribed to differences in the study protocols of the different studies. Therefore Table 1 also presents details on the study protocols used in the different Ames test protocols. Nevertheless, the comparison in Table 1 and Fig. 8 reveals that the site of methylation affects the mutagenic potential with especially methylation at C4, C6, C9 and C11 increasing the mutagenic potential as compared to B[a]P especially for the point mutations detected by TA100, while methylation at C1, C2, C3, C5, C10 and C12 reduce the potential. Altogether, the mutagenic potencies of the tested monomethylated B[a]Ps observed in the present study appear to be in line with the values reported in the studies of Utesch et al. [25] and Flesher

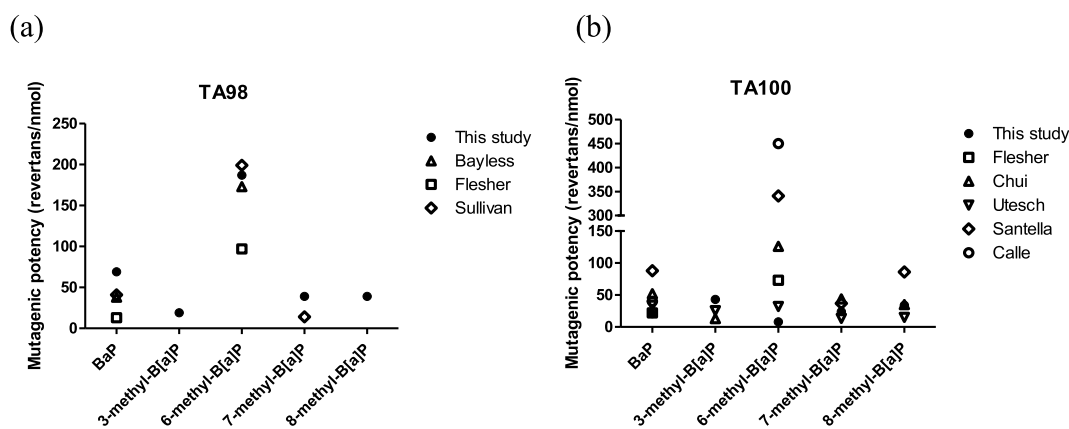


Fig. 8. Mutagenic potential for B[a]P and four of its monomethyl substituted analogues towards (a) TA98 and (b) TA100 in the reverse mutation test obtained from this study and literature data. Each symbol represents the mutagenic potential of the corresponding compound expressed in revertants/nmol. Note: the experimental conditions of bacterial reverse mutation assay may differ between studies.

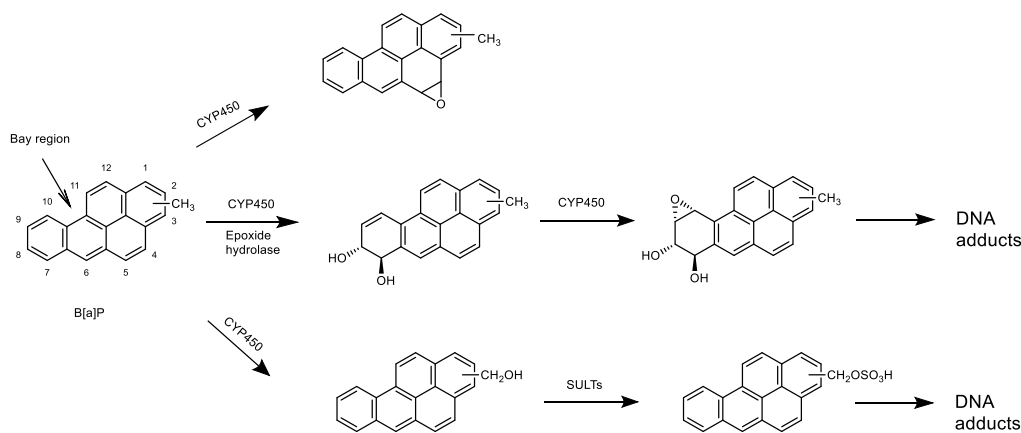


Fig. 9. Possible metabolic pathways for genotoxicity of monomethyl-substituted B[a]P.

et al. [27].

The dihydrodiol-epoxide pathway towards formation of the ultimate carcinogen 7,8-dihydrodiol-9,10-epoxide (Fig. 9) may be associated also with the carcinogenicity of monomethylated B[a]P analogues. The present study showed that 7,8-dihydrodiol, the metabolite that precedes the formation of the ultimate genotoxic metabolite 7,8-dihydrodiol-9,10-epoxide via the dihydrodiol-epoxide pathway, was detected at levels amounting to 7.8%, 5.8%, 7.4%, 1.0% and 0% of the total formation of metabolites for B[a]P, 3-methyl-, 6-methyl-, 7-methyl- and 8-methyl-B[a]P, respectively. This observation is in line with the reported skin tumor initiating activity of B[a]P and 3-methyl-B[a]P being potent, that of 6-methyl-B[a]P being weak, while 7-methyl- and 8-methyl-B[a]P for which the results of the present study indicate formation of the 7,8-dihydrodiol to be limited appeared inactive in the mouse skin painting assay (Table 1) [30]. The observed formation of 7,8-dihydrodiol also indicates that the dihydrodiol-epoxide pathway may be especially relevant for B[a]P, 3-methyl- and 6-methyl B[a]P. Considering the metabolites that may contribute to the mutagenicity it is of interest to note that previous studies have shown that, when tested in the Ames test with *S. typhimurium* tester strains TA98 and TA100 in the presence of metabolic activation, 7,8-dihydro-B[a]P-diol and B[a]P-4,5-oxide were more mutagenic than B[a]P itself [37,38]. It seems realistic to assume that not only the formation of 7,8-dihydrodiol but also the formation of 4,5-oxide metabolites from the methylated B[a]P analogues (Fig. 9) may play a role in their mutagenicity in the Ames test. For 1-methyl-, 6-methyl- and 7-methyl-B[a]P it was previously reported that their mutagenicity, as detected in the Ames test, remained unaffected by the addition of the epoxide hydrolase inhibitor trichloropropene oxide (TCPO), suggesting the role of the 7,8-dihydrodiol and the dihydrodiol-epoxide pathway to be perhaps somewhat limited [13,28]. Alternatively, 4,5-oxide metabolites of the monomethyl-B[a]Ps could possibly contribute to their in vitro mutagenicity because TCPO does not prevent the initial CYP450-mediated oxidation and epoxide hydrolase is well known to play a dual role in the mutagenicity of B[a]P in the Ames test [39]. In the liver S9 incubations (Fig. 8), the formation of 4,5-dihydrodiols, reflecting 4,5-oxide formation, ranged from 0.3% to 20% of the total metabolites formed for the four monomethylated B[a]Ps, indicating that the formation of a 4,5-oxide metabolite can be substantial and may possibly contribute to the mutagenic potential observed in the Ames test. It is expected that the 4,5-oxide of the monomethyl substituted B[a]Ps may be quickly converted by epoxide hydrolase and/or excreted in the in vivo situation, preventing the in vitro mutagenicity to be displayed in vivo. Furthermore, 6-hydroxymethyl-B[a]P, formed as a side chain metabolite that appeared to be formed at a level amounting to 4.9% of the total metabolites of 6-methyl-B[a]P, showed equivalent or higher mutagenic potency compared to 6-methyl-B[a]P in both TA98 and TA100 upon S9 metabolic activation suggesting that formation of a

mutagenic metabolite may even result from side chain oxidation [28]. Whether, in addition to this different potential to induce different type of mutations also differences in DNA repair mechanisms in the two tester strains add to this different response in the two tester strains remains to be elucidated. It also remains to be elucidated whether metabolites from side chain oxidation do play a role in the mutagenicity of other monomethylated B[a]P. The role of the meso-region side chain oxidation pathway was supported by in vivo studies. The methyl-substitution at the meso region of B[a]P, such as in 6-methyl-B[a]P, is suggested to result in methyl side chain oxidation to result in formation of 6-hydroxymethyl-B[a]P by CYP450 enzymes in the present study. Such benzylic alcohols of alkylated PAH like 6-hydroxymethyl-B[a]P can be metabolically converted by sulfotransferases (SULT) to reactive sulfate esters. This metabolic pathway leading to mutagenic intermediates is difficult to study in vitro in the standard Ames test as *Salmonella* strains are SULT-deficient and extracellular generated sulfate esters are not easily penetrating the plasma membrane as ionized metabolites [40]. Only genetically engineered *Salmonella typhimurium* strains expressing individual human and other mammalian SULT enzymes are useful tools to be applied in such studies [41,42]. However, studies in vivo have shown that benzylic alcohols like 6-hydroxymethyl-B[a]P could be conjugated by SULT to form the highly reactive 6-[(sulfoxy)methyl]-B[a]P [43]. Also in vivo studies suggested that this sulfate ester of 6-hydroxymethyl-B[a]P forms DNA adducts and represents an ultimate genotoxic metabolite based on guanine and adenine adducts that were formed in rats and mice [44–46]. It is also of interest that the tumorigenesis of 6-methyl-B[a]P may also relate to side chain oxidation as the benzylic ester of 6-hydroxymethyl-B[a]P was suggested to be the possible ultimate carcinogen in the in vivo mouse skin test [47].

However, within the series of the 12 monomethyl B[a]P compounds the 11-methyl isomer with the methyl group adjacent to the bay region is more tumorigenic than all other isomers or B[a]P itself [30]. The available data also with other PAHs indicate that the presence of a methyl group in the bay region obviously results in general in an increased tumorigenicity and that this structural motif allows the bay region dihydrodiol epoxides involved in the activation to more facile react with DNA [48–50].

Genotoxicity of the alkyl substituted PAHs is still to be elucidated with bioassays that are competent for human relevant metabolism of PAHs. Genotoxic potential of especially non alkylated PAHs has already been investigated using the γ H2AX in-cell western (ICW) assay and p53 reporter gene assay with human cell lines such as Hep 3B, LS-174, NCI-H358 and U2OS [51,52]. These assays may prove of value for future studies on the genotoxicity of alkylated PAHs. The discrepancies between observed tumor initiating activity in the mouse skin painting assay and mutagenicity in the bacterial reverse mutation assay can possibly be ascribed to the metabolic differences between species and

limitations of the current bacterial reverse mutation assay in comparison to the *in vivo* situation. The metabolism of B[a]P by mouse skin in the mouse skin painting assay could be different from the metabolism by rat and mouse liver CYP enzymes in the bacterial reverse mutation which may cause the discrepancy between the two assays. However, the metabolic profile by skin microsomes reported before appears to be comparable to that obtained for rat liver microsomes in the present study while quantitative differences between skin and liver metabolism of B[a]P may cause the discrepancy (Table S1 in supplementary materials) [23]. Another cause may be related to species differences in bioactivation of the methylated B(a)P analogues between mice and rats given that the skin painting assay is performed in mice and the liver S9 used in the Ames test generally comes from rats. Another reason potentially underlying the discrepancy may be the use of Arochlor 1254 induced liver S9 as compared to non-induced mouse skin. Moreover, the current bacterial reverse mutation assay lacks of expression of SULT that may play a role in the bioactivation of the methyl substituted B[a]Ps. Furthermore, considering the possible bioactivation of PAHs by SULTs, it would be of interest to test the genotoxicity of the PAHs in cell models engineered to express different human enzymes including relevant CYPs and SULTs, such as for example the V79 cells engineered to express CYP1A2 and SULT1A1 [53]. Use of these cell lines was already reported to result in predictions of the mutagenic potency of PAH diol epoxides that correlated better with the activity in rodent bioassays for carcinogenicity than Ames test results [54].

5. Conclusion

The present study concludes that methyl substitution of B[a]P may alter its mutagenic potency, with the actual effect, a relatively limited increase or decrease in mutagenic potential as compared to B[a]P itself, depending on the substituent position and the tester strain used. Methylation of B[a]P shifts the metabolism to alkyl side chain oxidation at the expense of aromatic ring oxidation, while elongation of the side chain reduces overall metabolism, the latter likely limiting metabolism and thus bioactivation via CYP450-mediated reactions with alkyl chains of 6 or more carbon atoms. The relevant pathways for mutagenicity and carcinogenicity of the selected monomethyl substituted B[a]P may involve the formation of a 7,8-dihydrodiol-9,10-epoxide, a 4,5-oxide and/or a benzylic alcohol as a side chain oxidative metabolite if it is converted to an unstable and reactive sulfate ester conjugate. It is concluded that alkylation of B[a]P does not systematically reduce its mutagenicity in spite of the metabolic shift from aromatic to side chain oxidation.

Funding information

This work was financially supported by Concawe (No. 201700093) in Belgium, and by a grant from China Scholarship Council from China (No. 201807720073) to Danlei Wang. Part of this work was supported by Operationeel Programma Kansen voor West II (EFRO) (project no KVV- 00181).

Author statement

Danlei Wang: Conceptualization, Formal analysis, Investigation, Methodology, Visualization, Writing-Original draft preparation. Angelique Groot: Methodology. Albrecht Seidel: Resources, Writing-Review & Editing. Lulu Wang: Investigation. Effimia Kiachaki: Investigation. Peter J. Boogaard: Conceptualization, Supervision, Writing – Review & Editing. Ivonne M.C.M. Rietjens: Conceptualization, Supervision, Writing – Review & Editing.

Declaration of competing interest

The authors declare that they have no known competing financial

interests or personal relationships that could have appeared to influence the work reported in this paper.

Appendix A. Supplementary data

Supplementary data to this article can be found online at <https://doi.org/10.1016/j.cbi.2022.110007>.

References

- [1] EFSA, Scientific Opinion on Mineral Oil Hydrocarbons in Food, EFSA Journal 10 (2012) 2704.
- [2] K. Grob, Mineral oil hydrocarbons in food: a review, Food Addit. Contam. Part A Chem Anal Control Expo Risk Assess 35 (2018) 1845–1860.
- [3] R. Pirow, A. Blume, N. Hellwig, M. Herzler, B. Huhse, C. Hutzler, K. Pfaff, H. J. Thierse, T. Tralau, B. Vieth, A. Luch, Mineral oil in food, cosmetic products, and in products regulated by other legislations, Crit. Rev. Toxicol. 49 (2019) 742–789.
- [4] B.M. Buijtenhuijs, Mineral Oils in Food; a Review of Occurrence and Sources, 2019.
- [5] C.R. Mackerer, L.C. Griffiths, J.S. Grabowski Jr., F.A. Reitman, Petroleum mineral oil refining and evaluation of cancer hazard, Appl. Occup. Environ. Hyg 18 (2003) 890–901.
- [6] IARC, benzo[a]pyrene, Chemical Agents and Related Occupations, International Agency for Research on Cancer, Lyon, France, 2012, pp. 111–138.
- [7] D.M. Jerina, J.M. Sayer, D.R. Thakker, H. Yagi, W. Levin, A.W. Wood, A.H. Conney, Carcinogenicity of Polycyclic Aromatic Hydrocarbons: the Bay-Region Theory, Springer Netherlands, Dordrecht, 1980, pp. 1–12.
- [8] P. Sims, P.L. Grover, A. Swaisland, K. Pal, A. Hewer, Metabolic activation of benzo[a]pyrene proceeds by a diol-epoxide, Nature 252 (1974) 326–328.
- [9] S.C. Cheng, B.D. Hilton, J.M. Roman, A. Dipple, DNA adducts from carcinogenic and noncarcinogenic enantiomers of benzo[a]pyrene dihydrodiol epoxide, Chem. Res. Toxicol. 2 (1989) 334–340.
- [10] D. Wang, B. Bruyneel, L. Kamelia, S. Wesseling, I.M.C.M. Rietjens, P.J. Boogaard, In vitro metabolism of naphthalene and its alkylated congeners by human and rat liver microsomes via alkyl side chain or aromatic oxidation, Chem. Biol. Interact. 315 (2020), 108905.
- [11] T.K. Wong, P.L. Chiu, P.P. Fu, S.K. Yang, Metabolic study of 7-methylbenzo[a]pyrene with rat liver microsomes: separation by reversed-phase and normal-phase high performance liquid chromatography and characterization of metabolites, Chem. Biol. Interact. 36 (1981) 153–166.
- [12] T. Kinoshita, M. Konieczny, R. Santella, A.M. Jeffrey, Metabolism and covalent binding to DNA of 7-methylbenzo[a]pyrene, Cancer Res. 42 (1982) 4032–4038.
- [13] T.K.W. Peilu Chiu, Peter P. Fu, Shen K. Yang, 7-methylbenzo[a]pyrene and Benzo[a]pyrene: Comparative Metabolic Study and Mutagenicity Testing in Salmonella Typhimurium TA100, Polynuclear Aromatic Hydrocarbons: Physical and Biological Chemistry, 1982, pp. 183–191.
- [14] P.D. Sullivan, I.J. Ocasio, J.D. Kittle, L.E. Ellis, The effect of antioxidants on the mutagenicity of benzo[a]pyrene and derivatives, in: A.B.A.J. Dennis (Ed.), Polynuclear Aromatic Hydrocarbons: Chemistry and Biological Effects, Battelle Press, Columbus, Ohio, 1980, pp. 163–175.
- [15] P.D. Sullivan, L.M. Calle, L.E. Ellis, L.M. Calle, I.J. Ocasio, Chemical and enzymatic oxidation of alkylated benzo[a]pyrenes, Chem. Biol. Interact. 40 (1982) 177–191.
- [16] K.L. Hamernik, Chiu, Pei Lu, Ming W. Chou, Peter P. Fu, Shen K. Yang, Metabolic activation of 6-methylbenzo[a]pyrene, in: M.D. Cooke, J. Anthony (Eds.), Polynuclear Aromatic Hydrocarbons, 1983.
- [17] K.L. Hamernik, The Comparative Study of the Metabolism of 6-methylbenzo[a]pyrene and Benzo[a]pyrene by Rat Liver Microsomes, Uniformed Services University of the Health Sciences, Bethesda, Maryland, 1984.
- [18] M.E. Staretz, S.E. Murphy, C.J. Patten, M.G. Nunes, W. Koehl, S. Amin, L.A. Koenig, F.P. Guengerich, S.S. Hecht, Comparative metabolism of the tobacco-related carcinogens benzo[a]pyrene, 4-(Methylnitrosamino)-1-(3-pyridyl)-1-butanone, 4-(Methylnitrosamino)-1-(3-pyridyl)-1-butanol, and N'-Nitrosornicotine in human hepatic microsomes, Drug Metabol. Dispos. 25 (1997) 154–162.
- [19] D. Wang, M.H. Rietdijk, L. Kamelia, P.J. Boogaard, I.M.C.M. Rietjens, Predicting the *in vivo* developmental toxicity of benzo[a]pyrene (BaP) in rats by an *in vitro-in silico* approach, Arch. Toxicol. 95 (2021) 3323–3340.
- [20] P. Sims, The metabolism of benzo[a]pyrene by rat-liver homogenates, Biochem. Pharmacol. 16 (1967) 613–618.
- [21] M.C. MacLeod, W. Levin, A.H. Conney, R.E. Lehr, B.K. Mansfield, D.M. Jerina, J. K. Selkirk, Metabolism of benzo(e)pyrene by rat liver microsomal enzymes, Carcinogenesis 1 (1980) 165–173.
- [22] J.K. Selkirk, R.G. Croy, J.P. Whitlock Jr., H.V. Gelboin, In vitro metabolism of benzo(a)pyrene by human liver microsomes and lymphocytes, Cancer Res. 35 (1975) 3651–3655.
- [23] M.H. Bickers, D. R. S.K. Yang, Metabolism of Benzo[a]pyrene by Skin Microsomes: Comparative Studies in C57BL/6N and DBA/2N Mice and Sprague-Dawley Rats, Polynuclear Aromatic Hydrocarbons: Physical and Biological Chemistry, 1982, pp. 121–131.
- [24] S.K.Y. Peilu Chui, A Structure-Activity Relationship Study of Monomethylbenzo[a]pyrenes by the Use of Salmonella Typhimurium Tester Strain TA100 and by Analysis of Metabolite Formation, Polynuclear Aromatic Hydrocarbons: Physical and Biological Chemistry, 1982, pp. 193–200.

- [25] D. Utesch, H. Glatt, F. Oesch, Rat hepatocyte-mediated bacterial mutagenicity in relation to the carcinogenic potency of benz(a)anthracene, benzo(a)pyrene, and twenty-five methylated derivatives, *Cancer Res.* 47 (1987) 1509–1515.
- [26] R. Santella, T. Kinoshita, A.M. Jeffrey, Mutagenicity of some methylated benzo[a]Pyrene derivatives, *Mutat. Res.* 104 (1982) 209–213.
- [27] A.M.K.J.W. Flesher, M. Chien, K.H. Stansbury, C. Gairola, K.L. Sydnor, Metabolic activation of carcinogenic hydrocarbons in the meso position (L region), in: M.C.A. J. Dennis (Ed.), *Polycyclic Aromatic Hydrocarbons: Formation, Metabolism and Measurement*, Battelle Press, 1983, pp. 505–515.
- [28] J.H. Bayless, J.E. Jablonski, S.M. Roach, P.D. Sullivan, Inhibition of the mutagenicity and metabolism of 6-methyl-benzo[a]pyrene and 6-hydroxymethyl-benzo[a]pyrene, *Biochem. Pharmacol.* 35 (1986) 2313–2322.
- [29] L.M. Calle, P.D. Sullivan, M.D. Nettleman, L.J. Ocasio, J. Blazyk, J. Jollick, Antioxidants and the mutagenicity of benzo(a) pyrene and some derivatives, *Biochem. Biophys. Res. Co* 85 (1978) 351–356.
- [30] R.P. Iyer, J.W. Lyga, J.A. Secrist 3rd, G.H. Daub, T.J. Slaga, Comparative tumor-initiating activity of methylated benzo(a)pyrene derivatives in mouse skin, *Cancer Res.* 40 (1980) 1073–1076.
- [31] D. Li, Y. Han, X. Meng, X. Sun, Q. Yu, Y. Li, L. Wan, Y. Huo, C. Guo, Effect of regular organic solvents on cytochrome P450-mediated metabolic activities in rat liver microsomes, *Drug Metab. Dispos.* 38 (2010) 1922–1925.
- [32] A. Hamel, M. Roy, R. Proudlock, Chapter 4 - the bacterial reverse mutation test, in: R. Proudlock (Ed.), *Genetic Toxicology Testing*, Academic Press, Boston, 2016, pp. 79–138.
- [33] H. Lee, J. Sheth, R.G. Harvey, Synthesis of putative oxidized metabolites of 8-methylbenzo[a]pyrene, *Carcinogenesis* 4 (1983) 1297–1299.
- [34] D. Wang, V. Schramm, J. Pool, E. Pardali, A. Brandenburg, I.M.C.M. Rietjens, P. J. Boogaard, The effect of alkyl substitution on the oxidative metabolism and mutagenicity of phenanthrene, *Arch. Toxicol.* 96 (2022) 1109–1131.
- [35] L. Kamelia, L. de Haan, B. Spenkelink, B. Bruyneel, H.B. Ketelslegers, P. J. Boogaard, I.M.C.M. Rietjens, The role of metabolism in the developmental toxicity of polycyclic aromatic hydrocarbon-containing extracts of petroleum substances, *J. Appl. Toxicol.* 40 (2020) 330–341.
- [36] A.V. Heyst, Mineral Oil Migration from Cardboard Food Contact Materials: Hazard Identification and Exposure Assessment of the Belgian Population, *Vrije Universiteit Brussel*, Brussel, 2019.
- [37] A.W. Wood, W. Levin, A.Y.H. Lu, D. Ryan, S.B. West, H. Yagi, H.D. Mah, D. M. Jerina, A.H. Conney, Structural requirements for metabolic activation of benzo[a]Pyrene to mutagenic products - effects of modifications in 4,5-positions, 7,8-positions, and 9,10-positions, *Mol. Pharmacol.* 13 (1977) 1116–1125.
- [38] P.G. Wislocki, A.W. Wood, R.L. Chang, W. Levin, H. Yagi, O. Hernandez, D. M. Jerina, A.H. Conney, High mutagenicity and toxicity of a diol epoxide derived from benzo(a)pyrene, *Biochem. Biophys. Res. Commun.* 68 (1976) 1006–1012.
- [39] P. Bentley, F. Oesch, H. Glatt, Dual role of epoxide hydratase in both activation and inactivation of benzo(a)Pyrene, *Arch. Toxicol.* 39 (1977) 65–75.
- [40] H. Glatt, A. Seidel, R.G. Harvey, M.W. Coughtrie, Activation of benzylic alcohols to mutagens by human hepatic sulphotransferases, *Mutagenesis* 9 (1994) 553–557.
- [41] W. Meinel, C. Tsoi, S. Swedmark, Z.E. Tibbs, C.N. Falany, H. Glatt, Highly selective bioactivation of 1- and 2-hydroxy-3-methylcholanthrene to mutagens by individual human and other mammalian sulphotransferases expressed in *Salmonella typhimurium*, *Mutagenesis* 28 (2013) 609–619.
- [42] C. Bendadani, W. Meinel, B. Monien, G. Dobbernack, S. Florian, W. Engst, T. Nolden, H. Himmelbauer, H. Glatt, Determination of sulphotransferase forms involved in the metabolic activation of the genotoxicant 1-hydroxymethylpyrene using bacterially expressed enzymes and genetically modified mouse models, *Chem. Res. Toxicol.* 27 (2014) 1060–1069.
- [43] J.W. Flesher, J. Horn, A.F. Lehner, 6-sulfooxymethylbenzo[a]pyrene is an ultimate electrophilic and carcinogenic form of the intermediary metabolite 6-hydroxymethylbenzo[a]pyrene, *Biochem. Biophys. Res. Commun.* 234 (1997) 554–558.
- [44] K.H. Stansbury, J.W. Flesher, R.C. Gupta, Mechanism of aralkyl-DNA adduct formation from benzo[a]pyrene in vivo, *Chem. Res. Toxicol.* 7 (1994) 254–259.
- [45] E.G. Rogan, A. Hakam, E.L. Cavalieri, Structure elucidation of a 6-methylbenzo[a]pyrene-DNA adduct formed by horseradish peroxidase in vitro and mouse skin in vivo, *Chem. Biol. Interact.* 47 (1983) 111–122.
- [46] J.W. Flesher, K.L. Sydnor, Possible role of 6-hydroxymethylbenzo(a)pyrene as a proximate carcinogen of benzo(a)pyrene and 6-methylbenzo(a)pyrene, *Int. J. Cancer* 11 (1973) 433–437.
- [47] E. Cavalieri, R. Roth, C. Grandjean, J. Althoff, K. Patil, S. Liakus, S. Marsh, Carcinogenicity and metabolic profiles of 6-substituted benzo[a]pyrene derivatives on mouse skin, *Chem. Biol. Interact.* 22 (1978) 53–67.
- [48] P.G. Wislocki, K.M. Fiorentini, P.P. Fu, S.K. Yang, A.Y. Lu, Tumor-initiating ability of the twelve monomethylbenzo[a]anthracenes, *Carcinogenesis* 3 (1982) 215–217.
- [49] S.S. Hecht, A. Meilikian, S. Amin, Effects of methyl substitution on the tumorigenicity and metabolic activation of polycyclic aromatic hydrocarbons, in: S.K. Yang, B.D. Silverman (Eds.), *Polycyclic Aromatic Hydrocarbon Carcinogenesis: Structure-Activity Relationships*, CRC Press, Boca Raton, FL, 1988, pp. 95–128.
- [50] J.M. Lin, D. Desai, L. Chung, S.S. Hecht, S. Amin, Synthesis of anti-7,8-dihydroxy-9,10-epoxy-7,8,9, 10-tetrahydro-11-methylbenzo[a]pyrene and its reaction with DNA, *Chem. Res. Toxicol.* 12 (1999) 341–346.
- [51] S.C. van der Linden, A.R. von Bergh, B.M. van Vught-Lussenburg, L.R. Jonker, M. Teunis, C.A. Krul, B. van der Burg, Development of a panel of high-throughput reporter-gene assays to detect genotoxicity and oxidative stress, *Mutat. Res. Genet. Toxicol. Environ. Mutagen* 760 (2014) 23–32.
- [52] F. Tomasetti, C. Tebbi, V. Graillet, F. Zeman, A. Pery, J.P. Cravedi, M. Audebert, Comparative genotoxic potential of 27 polycyclic aromatic hydrocarbons in three human cell lines, *Toxicol. Lett.* 326 (2020) 99–105.
- [53] A. Seidel, T. Friedberg, B. Lollmann, A. Schwierzok, M. Funk, H. Frank, R. Holler, F. Oesch, H. Glatt, Detoxification of optically active bay- and fjord-region polycyclic aromatic hydrocarbon dihydrodiol epoxides by human glutathione transferase P1-1 expressed in Chinese hamster V79 cells, *Carcinogenesis* 19 (1998) 1975–1981.
- [54] M. Chevereau, H. Glatt, D. Zalko, J.P. Cravedi, M. Audebert, Role of human sulphotransferase 1A1 and N-acetyltransferase 2 in the metabolic activation of 16 heterocyclic amines and related heterocyclics to genotoxins in recombinant V79 cells, *Arch. Toxicol.* 91 (2017) 3175–3184.